Vibrational Energy Relaxation of S 1 Perylene in Solution

ARTICLE *in* THE JOURNAL OF PHYSICAL CHEMISTRY A · APRIL 2004

Impact Factor: 2.69 · DOI: 10.1021/jp036503j

Vibrational Energy Relaxation of S_1 Perylene in Solution

Tatsuya Kasajima,[†] Seiji Akimoto,[‡] Shin-ichiro Sato,* and Iwao Yamazaki[§]

Department of Molecular Chemistry, Graduate School of Engineering, Hokkaido University, Sapporo 060-8628, Japan

Received: August 22, 2003; In Final Form: January 21, 2004

Vibrational energy relaxations of S_1 perylene and S_1 12-(3-perylenyl)dodecanoic acid (PD) in 2-methyltetrahydrofuran at room temperature were investigated by using a Franck−Condon analysis of femtosecond time-resolved fluorescence spectra. Vibrational energy relaxation from $|2\rangle$, $v' = 2$ level of ν_7 mode, occurs not only via successive route, $|2\rangle \rightarrow |1\rangle$ followed by $|1\rangle \rightarrow |0\rangle$, but also via direct route, $|2\rangle \rightarrow |0\rangle$. The vibrational energy relaxation times were obtained as 2.7 ps for $|2\rangle \rightarrow |1\rangle$, 1.8 ps for $|1\rangle \rightarrow |0\rangle$, and 700 fs for $|2\rangle \rightarrow |0\rangle$ in perylene and 1.9 ps for $|2\rangle \rightarrow |1\rangle$, 1.2 ps for $|1\rangle \rightarrow |0\rangle$, and 500 fs for $|2\rangle \rightarrow |0\rangle$ in PD. An average-matrix-element treatment proposed by Fourmann et al. (*Chem. Phys.* **1985**, *92*, 25) was employed to account for these relaxation times in the Fermi's golden rule. Two parameters of the average-matrix element were estimated to be $V_0 = 0.59$ cm^{-1} and $0.46 < \alpha < 0.55$ in our analysis, which were in reasonable agreement with Fourmann's analysis, $V_0 = 0.65$ cm^{-1} and $\alpha = 0.3$, for fluorescence spectra of perylene in supersonic jet. To discuss the energy flow in the ν_7 mode, transient vibrational temperatures were also calculated at each time. "Intramode" thermal equilibriums in the ν_7 mode both for perylene and for PD are not established while the vibrational temperature is higher than room temperature.

1. Introduction

Dissipation of excess vibrational energy plays an important role in photochemical reactions in condensed phase and hence has attracted considerable attention of researchers. A number of experimental and theoretical studies were reported to understand the mechanism of vibrational energy relaxation (VER).[1−15] Vibrational energy relaxation has both intra- and intermolecular processes in solution. The intramolecular processes are called intramolecular vibrational redistribution (IVR) rather than intramolecular vibrational relaxation, because the vibrational energy initially deposited on Franck−Condon active modes of a molecule is conserved within the molecule during the course of the intramolecular processes. On the other hand, the intermolecular processes are often called as vibrational cooling (VC) or intermolecular energy transfer, because the vibrational energy is transferred from the solute molecule to solvent molecules as thermal energy. It was generally accepted that VER for a polyatomic molecule in solution proceeds as follows. Immediately after photoexcitation, very rapid randomization of an excess vibrational energy is completed within subpicoseconds as a result of IVR, which creates thermal equilibrium in the solute molecule. At this stage, the solute molecule has a common mode-independent vibrational temperature, which is, however, higher than that of surrounding solvent molecules. The vibrationally hot molecule then dissipates its excess vibrational energy into surrounding solvent molecules through VC on the time scale of 1−100 ps. This picture of VER has come mainly from ultrafast transient absorption and fluorescence studies. However, recent various time-resolved spectroscopic studies of large molecules in solution have shown the existence of slow IVR in a few picoseconds time scale as well as fast IVR in subpicoseconds time scale.[1−13] In the slow IVR, dynamics will be complex because the time scale of IVR becomes closer to that of VC. From those recent experimental results, the VER process in solution would not be clearly divided into two temporally distinct steps (i.e., IVR and VC).

Vibrational energy relaxation of porphyrins in solution were studied in detail.[1−5] Akimoto et al. have examined energy relaxation processes of 5,15-bis(3,5-di-*tert*-butylphenyl)-21*H*,23*H*-porphine (H_2DDTBPP) and 5,15-bis(3,5-di-*tert*-butylphenyl)zinc porphine (ZnDDTBPP) in benzene by using a femtosecond fluorescence up-conversion method.[1] They found the time scales associated with the VER processes following B band excitation of H_2DDTBPP and ZnDDTBPP: 1.5 ps for H_2DDTBPP in the Q_x state and 600 fs for ZnDDTBPP in the Q state. Baskin et al. have studied free-base tetraphenylporphyrin (H_2TPP) in benzene by using the femtosecond fluorescence up-conversion method and a pump−probe transient absorption with femtosecond resolution.[2] They found three relaxation times as follows: 100−200 fs, 1.4 ps, and 10−20 ps. The fastest component of 100−200 fs was assigned to IVR in the Q_x state and the slowest component of 10−20 ps was correlated with VC. For the middle component of 1.4 ps, they interpreted as vibrational redistribution caused by elastic or quasi-elastic collisions with solvent molecules. In this relaxation process no or little vibrational energy flows from solute molecules to solvent molecules, though vibrational redistribution is enhanced by collisions with solvents. Sato and Kitagawa have studied nickel octaethylporphyrin (NiOEP) in the (d, d) excited state in solution by time-resolved anti-Stokes Raman spectroscopy.[3] They found (1) that transient vibrational temperatures of ν_4 and ν_7 modes within 10 ps are higher than calculated intramolecular vibrational temperature (473 K) at thermal equilibrium with

* Corresponding author. Phone: 81-11-706-6607. Fax: 81-11-709-2037. E-mail: s-sato@eng.hokudai.ac.jp.
[†] E-mail: kasajima@mm3-mc.eng.hokudai.ac.jp.
[‡] E-mail: akimoto@eng.hokudai.ac.jp.
[§] E-mail: yamiw@eng.hokudai.ac.jp.

10.1021/jp036503j CCC: $27.50
Published on Web 00/00/0000 PAGE EST: 7.8

equipartitioning of the excess vibrational energy and (2) that the transient vibrational temperature of the ν_4 mode (>754 K) is higher than that of the ν_7 mode (>570 K) within 10 ps. These results indicate that IVR is not completed in a few picoseconds time scale following photoexcitation. Mizutani et al. have investigated NiOEP in the (d, d) excited state in benzene by time-resolved anti-Stokes Raman spectroscopy.[4] They found that the rise of anti-Stokes ν_7 intensity is delayed by 2.6 ± 0.5 ps, although the rise of anti-Stokes ν_4 intensity is instantaneous. This is direct evidence that IVR has not been completed within subpicoseconds.

Vibrational energy relaxation of S_1 *trans*-stilbene in solution was also investigated in detail.[6−8] Two research groups have reported anti-Stokes Raman spectra of S_1 *trans*-stilbene with excess vibrational energy in solution.[7,8] Qian et al. have concluded that a nonstatistical distribution of excess vibrational energy among intramolecular vibrational modes persists for several picoseconds after photoexcitation on the basis of an analysis of temporal behavior of the anti-Stokes Raman intensities.[7] Nakabayashi et al. have also reached the same conclusion that IVR is not completed within initial few picoseconds and have obtained another result that almost no transients were populated at higher vibrational levels ($v' \geq 2$) in S_1 *trans*-stilbene a few picoseconds after photoexcitation, though *trans*-stilbene was excited to S_1 with a large excess vibrational energy of $\sim$5200 cm^{-1}.[8] From these results they have suggested that IVR of S_1 *trans*-stilbene proceeds in roughly two steps; that is, S_1 *trans*-stilbene with such high excess vibrational energy of $\sim$5200 cm^{-1} relaxes very rapidly (probably within subpicoseconds) to the lowest vibrationally excited levels (i.e., $v' = 1$) in the S_1 state, and then slower relaxation (in several picoseconds) occurs.

In the present paper, we present the results of a Franck−Condon (FC) analysis of time-resolved fluorescence spectra of S_1 perylene and S_1 12-(3-perylenyl)dodecanoic acid (PD) in 2-methyltetrahydrofuran (MTHF) after photoexcitation with an excess vibrational energy of $\sim$2800 cm^{-1} ($v' = 2$ level of ring-breathing mode). Meyer and Plaza have measured time-resolved absorption spectra of perylene in the S_1 state in cyclohexane.[16] When perylene is excited at 425 nm (the overtone of the 352 cm^{-1} mode), a transient peak appears at 489 nm, though this peak is not observed after 435 nm excitation (0−0 transition). The peak was assigned to stimulated emission from hot vibrational levels that relax with $\sim$1 ps decay constant. Though there are other reports[17−20] on VER of perylene in various solutions, the dynamics of thermal equilibration processes of perylene in solution are not yet fully understood. We have chosen perylene and PD as sample molecules for the following two reasons. First, each of these molecules has a clear vibrational progression due to a ring-breathing mode and, therefore, is suited to the FC analysis. Second, a comparison of the VER rates of perylene with those of PD helps us to classify the observed VER into an intramolecular or an intermolecular process. Smalley and co-workers have studied substituent effects on IVR in the gas phase.[21] These studies have ascertained that the more the density of vibrational states increases, the faster IVR rates become. Therefore, the observed VER would be considered as IVR, if the VER rate of PD were faster than that of perylene, because the IVR rate is generally accelerated by an increase of the density of vibrational states. On the other hand, the observed VER would be regarded as VC if the VER rates of perylene and PD were very close.

From recent experimental results for porphyrins, *trans*-stilbene, and so on, it is obvious that "intermode" thermal equilibriums require at least a few picoseconds time scale. However, these experimental results have not yet cleared time scales of "intramode" thermal equilibriums at all. We have previously reported an "intramode" thermal relaxation processes of S_1 perylene and S_1 PD in solution at room temperature.[13] Further results of analysis for the "intramode" thermal relaxation processes of those molecules are described in the present paper, which provides novel insight on VER in "intramode" when polyatomic molecules in solution are excited at higher vibrational levels ($v' \geq 2$).

2. Experimental Section

Perylene and PD were purchased from Sigma Chemical Co. and Molecular Probes Co., respectively, and used without further purification. 2-Methyltetrahydrofuran was purchased from Merck and used after distillation. Steady-state absorption and fluorescence spectra were measured with a JASCO Ubest-50 spectrophotometer and a Hitachi F-4500 fluorescence spectrometer, respectively. The concentrations of sample solutions were $\sim 10^{-5}$ M for the steady-state absorption measurements and $\sim 10^{-6}$ M for the steady-state fluorescence measurements, respectively.

Fluorescence-decay curves were measured with a femtosecond fluorescence up-conversion system using a Ti:Sapphire laser (Tsunami, Spectra-Physics) that was pumped with a diode-pumped solid-state laser (Millennia Xs, Spectra-Physics). The details of this system were described elsewhere.[9] Briefly, the near-IR pulses (776 nm, 80 MHz for perylene and 786 nm, 80 MHz for PD) were separated into two by a beam splitter; one was frequency-doubled by a BBO crystal and used to excite the sample, whereas the other near-IR beam served as a gate pulse. The gate pulse traversed a variable delay before being combined with the fluorescence in a BBO crystal whereas the excitation pulse traversed a fixed delay before being focused into a 1 mm sample cell. To avoid polarization effects, the angle between polarizations of the excitation beam and the probe beam was set to the magic angle by a $\lambda/2$ plate. Fluorescence-decay curves were measured at 17 points between 422 and 536 nm for perylene (filled circle in Figure 1a) and at 18 points between 431 and 558 nm for PD (filled circle in Figure 1b). The concentrations of perylene and PD solutions used for the fluorescence-decay-curve measurements were $\sim 10^{-5}$ M. All experiments were carried out in MTHF solution at room temperature ($\sim$295 K).

Each fluorescence-decay curve was deconvoluted by an iterative method. In this analysis, a Gaussian function fitted to the up-conversion signal from the pure solvent Raman scattering was used as an instrumental response function whose temporal width was estimated to be 200 fs. For all the monitoring wavelengths, the integrated intensities of fluorescence-decay curves were normalized to the steady-state fluorescence spectrum. Time-resolved fluorescence spectra were reconstructed by using these normalized fluorescence-decay curves.

3. Results and Discussion

3.1. Steady-State Absorption and Fluorescence Spectra. Steady-state absorption and fluorescence spectra are shown in Figure 1a for perylene and in Figure 1b for PD. The absorption and fluorescence spectra of PD are very similar to those of perylene except for spectral red shifts. The peak positions of vibrational bands of PD were red-shifted about 6 nm from those of perylene in the absorption spectrum, and about 10 nm in the fluorescence spectrum. The S_0 and S_1 potential curves both in

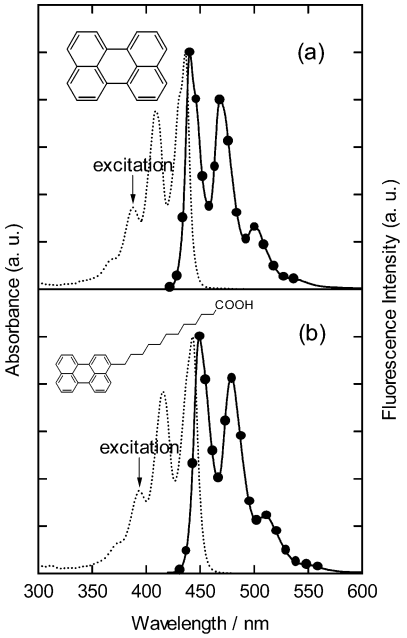

Figure 1. Steady-state absorption (dotted line) and fluorescence (solid line) spectra of (a) perylene and (b) PD in MTHF. The excitation wavelengths are 388 and 393 nm for perylene and PD, respectively. Filled circles on the fluorescence spectra indicate the measured wavelengths of time-resolved fluorescence spectra. Inset: molecular structures of perylene and PD.

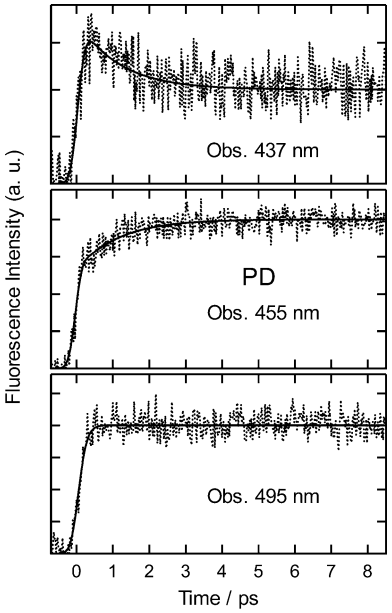

Figure 2. Typical fluorescence rise and decay curves measured with a femtosecond fluorescence up-conversion method observed at indicated wavelengths for PD in MTHF. The excitation wavelength is 393 nm. Each fluorescence-decay curve was deconvoluted with an instrumental response function of 200 fs fwhm, and then fitted to a sum of exponential terms, $\sum A_i \exp(-t/\tau_i)$, with independent amplitudes, A^i, and lifetimes, τ_i. Solid lines are fits of the experimental data.

perylene and in PD may be safely modeled as displaced harmonic oscillators because their absorption and fluorescence spectra are mirror images. It seems that the vibrational bands in the absorption and fluorescence spectra of perylene and PD at room temperature are apparently composed of a single vibrational mode, but these bands are combination bands composed of the ν_7 (1375 cm^{-1} in the S_0 state of perylene in *n*-hexane) and ν_{15} (358 cm^{-1} in the S_0 state of perylene in *n*-hexane) modes.[17] For simplicity, we treated the vibrational bands in the absorption and fluorescence spectra as a single vibrational progression of the ν_7 mode in the FC analysis of time-resolved fluorescence spectra.

3.2. Time-Resolved Fluorescence Spectra. Each fluorescence-decay curve was deconvoluted by an iterative method using an instrumental response function whose temporal width was estimated to be 200 fs. Typical rise and decay curves of PD are shown in Figure 2.

The molecules excited to the higher vibrational levels of the S_1 state may experience both VER and the fluorescence emission simultaneously. The steady-state fluorescence spectrum contains almost no emission components from the higher vibrational levels because the lifetimes (approximately nanoseconds) of fluorescence emission of aromatic organic compounds are usually much longer than the VER times (approximately picoseconds).

In contrast, the time-resolved fluorescence spectra contain many emission components from the higher vibrational levels in S_1 when the molecules are initially excited to the higher vibrational levels. The time-resolved fluorescence spectra contain emissions from the higher vibrational levels at $\upsilon' = 1$, 2 in S_1 because the molecules were excited to the $\upsilon' = 2$ level in S_1. Therefore, the difference spectra in Figure 3 reflect the overall vibrational relaxation from $\upsilon' = 1$, 2. A vibrational population at each vibrational level may be estimated if the contribution of emissions from the higher vibrational levels (υ' = 1, 2) are extracted separately from the time-resolved fluorescence spectra by the FC analysis.

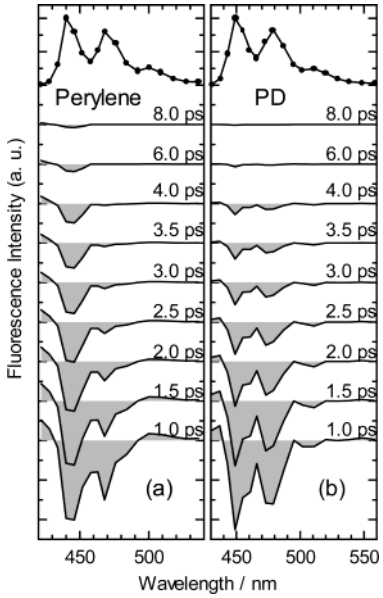

Figure 3. Time-resolved difference spectra of (a) perylene and (b) PD in MTHF at the indicated delay times, which were obtained by subtracting the steady-state fluorescence spectra from the time-resolved fluorescence spectra. The steady-state fluorescence spectra are shown at the top. Time constants, 1.9−2.4 ps for perylene and 1.1−1.4 ps for PD depending on the measured wavelengths, were obtained as a result of analyzing the fluorescence rise and decay curves.

3.3. Franck−Condon Analysis. The vibrational progressions of fluorescence from the higher vibrational levels ($\upsilon' = 1$, 2) have to be determined to obtain the fractions of emission from the higher vibrational levels ($\upsilon' = 1$, 2). These progressions are estimated from the steady-state fluorescence spectrum by assuming the displaced harmonic oscillator model on the S_0 and S_1 potential surfaces. In the displaced harmonic oscillator mo-

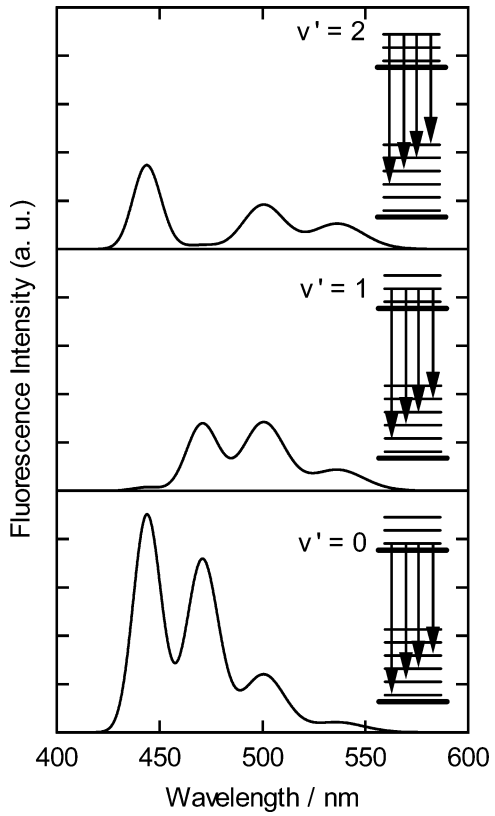

Figure 4. Component spectra (the vibrational progressions of the fluorescence from $v' = 0$, 1 and 2) of perylene calculated by eq 1 with $D = 1.5$.

del, vibrational progressions can be given by the following equation:[22]

$$I(m,n) \propto \nu_{mn}{}^4\{2^{-(m+n)}m!n!\} \exp\left(-\frac{D^2}{2}\right) \left\{\sum_{r=0}^{\min(m,n)} \frac{2^r D^{m+n-2r}(-1)^{n-r}}{r!(m-r)!(n-r)!}\right\}^2 \quad (1)$$

In eq 1 $I(m,n)$ is the relative intensity of the fluorescence from $v' = m$ to $v = n$, ν_{mn} is a vibronic transition energy between $v' = m$ and $v = n$, and D is a nondimensional potential displacement between S_0 and S_1. The displacement, D, was adjusted to reproduce the vibrational progression of the steady-state fluorescence that originates almost from $v' = 0$ by using eq 1. The displacement was thus determined as $D = 1.5$ both for perylene and for PD. This D value was used to obtain the vibrational progressions of the fluorescence from $v' = 1$, 2 in eq 1, that is, $I(1,n)$ and $I(2,n)$. The component spectra (the vibrational progressions from $v' = 0$, 1 and 2) of perylene are shown in Figure 4. Four peak intensities ($n \rightarrow n$, $n \rightarrow n + 1$, $n \rightarrow n + 2$, and $n \rightarrow n + 3$: $n = 0$, 1, 2) of a vibrational progression in a linear combination of the component spectra for $v' = 0$, 1, and 2 were fitted to those in a time-resolved fluorescence spectrum by least-squares method. For the positive peak around 420 nm in Figure 3, which may be assigned as a tail due to a hot band ($n \rightarrow n - 1$), we could not measure the accurate intensity due to the reabsorption effect. Therefore, we omitted the contribution from the $n \rightarrow n - 1$ band in our FC analysis.

The fraction of component spectra contained in each of the time-resolved fluorescence spectra may be regarded as the fraction of population at each vibrational level. Therefore,

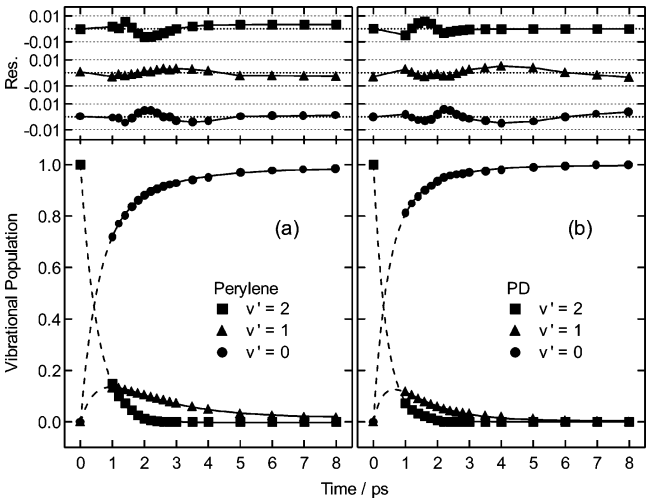

Figure 5. Vibrational populations of $v' = 0$, 1, and 2 at the indicated delay times for (a) perylene and (b) PD. Filled circles, filled triangles, and filled squares show vibrational populations of $v' = 0$, 1, and 2, respectively. Initial populations were assumed as $N_2 = 1$, $N_1 = N_0 = 0$ at $t = 0$ on the basis of kinetic model described in the text. The residuals for each fitting curve are shown in the upper windows.

relative vibrational population fractions of $v' = 0$, 1, and 2 were obtained from the FC analysis and were plotted against delay time (Figure 5). Initial populations were assumed as $N_2 = 1$, $N_1 = N_0 = 0$ at $t = 0$, where $N_{v'}$ ($v' = 0$, 1, and 2) represents a normalized population of each vibrational level, on the basis of kinetic model described in Section 3.4.

3.4. Vibrational Energy Relaxation. Three schemes of VER were employed to fit populations at $v' = 0$, 1 and 2 (Figure 5). The first VER scheme (Scheme a) is the successive decay process in which the vibrational population at $|2\rangle$ successively relaxes from $|2\rangle$ to $|1\rangle$ and then from $|1\rangle$ to $|0\rangle$.

$$|2\rangle \xrightarrow{k_{21}} |1\rangle \xrightarrow{k_{10}} |0\rangle \quad \text{(a)}$$

The rate equations in the successive relaxation can be solved as follows:

$$N_2 = \mathrm{e}^{-k_{21}t} \quad (2)$$

$$N_1 = \frac{k_{21}}{k_{21} - k_{10}}\{-\mathrm{e}^{-k_{21}t} + \mathrm{e}^{-k_{10}t}\} \quad (3)$$

and

$$N_0 = 1 + \frac{k_{10}}{k_{21} - k_{10}}\mathrm{e}^{-k_{21}t} - \frac{k_{21}}{k_{21} - k_{10}}{}^{-k_{10}t} \quad (4)$$

where $N_{v'}$ ($v' = 0$, 1, and 2) represents a normalized population of each vibrational level with the initial conditions $N_2 = 1$, $N_1 = N_0 = 0$ at $t = 0$. The population of $|2\rangle$ for perylene was fitted with a single-exponential curve

$$N_2 = \mathrm{e}^{-1.903t} \quad (5)$$

and $k_{21} = 1.903$ is thus obtained. With the fixed value of $k_{21} = 1.903$, the population of $|0\rangle$ was fitted with double exponential curves

$$N_0 = 1 - 0.7119\mathrm{e}^{-1.903t} - 0.2774\mathrm{e}^{-0.5444t} \quad (6)$$

and $k_{10} = 0.5444$ is thus obtained. With these k values, however, preexponential factors in eq 4 become $k_{10}/(k_{21} - k_{10}) = 0.4007$

and $k_{21}/(k_{21} - k_{10}) = 1.401$. These values totally disagree with the corresponding coefficients in eq 6. Therefore, VER for perylene cannot be reproduced by the successive decay process (Scheme a). This conclusion is unchanged even if the initial population of $v' = 1$ is not zero at $t = 0$.

The second VER scheme (Scheme b) is the decay process in which the direct pass from $|2\rangle$ to $|0\rangle$ is added to Scheme a.

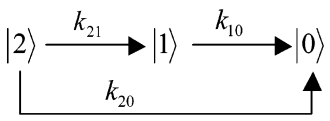

(b)

The rate equations in Scheme b can be solved as

$$N_2 = e^{-(k_{21}+k_{20})t} \tag{7}$$

$$N_1 = \frac{k_{21}}{(k_{21} + k_{20}) - k_{10}}\{-e^{-(k_{21}+k_{20})t} + e^{-k_{10}t}\} \tag{8}$$

and

$$N_0 = 1 + \frac{k_{10} - k_{20}}{(k_{21} + k_{20}) - k_{10}}e^{-(k_{21}+k_{20})t} - \frac{k_{21}}{(k_{21} + k_{20}) - k_{10}}e^{-k_{10}t} \tag{9}$$

From eqs 5 and 7, $k_{21} + k_{20}$ is obtained. By comparing the third term in eq 6 with that in eq 9, $k_{10} = 0.5444$ and $k_{21}/\{(k_{21} + k_{20}) - k_{10}\} = 0.2744$ are obtained. Therefore, $k_{21} = 0.3728$ and $k_{20} = 1.530$. The preexponential factor of the second term in eq 9 is $(k_{10} - k_{20})/\{(k_{21} + k_{20}) - k_{10}\} = -0.7255$ from these k values. This preexponential factor, -0.7255, agrees very well with the corresponding coefficient, -0.7119, in eq 6. The population for $|1\rangle$ is reconstructed by substituting these k values into eq 8 and the curve thus obtained reproduced the data for $|1\rangle$ very well, as shown in Figure 5a. Vibrational energy relaxation of perylene should occur through Scheme b including the direct relaxation pass from $|2\rangle$ to $|0\rangle$. However, the reason that Scheme b reproduced the data better than Scheme a might be due to simply increased numbers of variables used for fitting. That is why the third VER scheme (Scheme c) is tried to fit populations at $v' = 0$, 1, and 2.

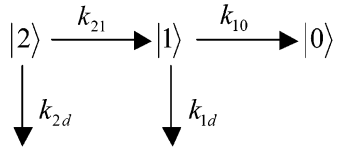

(c)

The rate equations in Scheme c can be solved as

$$N_2 = e^{-(k_{21}+k_{2d})t} \tag{10}$$

$$N_1 = \frac{k_{21}}{(k_{21}+k_{2d}) - (k_{10}+k_{1d})}\{-e^{-(k_{21}+k_{2d})t} + e^{-(k_{10}+k_{1d})t}\} \tag{11}$$

and

$$N_0 = 1 - \frac{k_{21}k_{10}}{\{(k_{21} + k_{2d}) - (k_{10} + k_{1d})\}(k_{21} + k_{2d})}e^{-(k_{21}+k_{2d})t} - \frac{k_{21}k_{10}}{\{(k_{21} + k_{2d}) - (k_{10} + k_{1d})\}(k_{10} + k_{1d})e^{-(k_{10}+k_{1d})t}} \tag{12}$$

From eqs 5 and 10, $k_{21} + k_{2d}$ is obtained. By comparing eq 6 with eq 12, $k_{10} + k_{1d}$ and the following values

$$\frac{k_{21}k_{10}}{\{(k_{21} + k_{2d}) - (k_{10} + k_{1d})\}(k_{21} + k_{2d})} = 0.7119 \tag{13}$$

and

$$\frac{k_{21}k_{10}}{\{(k_{21} + k_{2d}) - (k_{10} + k_{1d})\}(k_{10} + k_{1d})} = 0.2744 \tag{14}$$

are obtained. However, $k_{21}k_{10} = 1.841$ is calculated from eq 13, although $k_{21}k_{10} = 0.2030$ from eq 14. Therefore, it is obvious that Scheme c fail to reconstruct the experimental data. Vibrational energy relaxation of PD was also explained by Scheme b as a result of the same discussion above for perylene. The results of fitting to the vibrational populations ($v' = 0$, 1, and 2) with eqs 7−9 are shown in Figure 5. The VER rates of perylene and PD are summarized in Table 1.

TABLE 1: Vibrational Energy Relaxation Rates

	perylene	PD
k_{21}	0.37 ± 0.03 ps^{-1} (2.7 ± 0.2 ps)	0.54 ± 0.01 ps^{-1} (1.9 ± 0.1 ps)
k_{10}	0.54 ps^{-1} (1.8 ps)	0.82 ps^{-1} (1.2 ps)
k_{20}	1.53 ps^{-1} (700 fs)	2.03 ps^{-1} (500 fs)

Recently, VER of $SO(B^3\Sigma^-, v' = 1$ and 2) in the gas phase (He) was studied by Yamasaki et al.[23] They have found both $|2\rangle \rightarrow |1\rangle$ and $|2\rangle \rightarrow |0\rangle$ VER are similar to scheme b, and 15% of the relaxation from $v' = 2$ are the $|2\rangle \rightarrow |0\rangle$ type. In the present study, the $|2\rangle \rightarrow |0\rangle$ relaxations are 80% for perylene and 79% for PD. The larger vibrational degrees of freedom and/or the presence of solvent seem to accelerate the $|2\rangle \rightarrow |0\rangle$ relaxation.

3.5. Comparison with the Theoretical Vibrational Relaxation Rates. The experimental values of the VER rates were compared with the theoretical values given by Fermi's golden rule

$$w_{nm} = \frac{2\pi}{\hbar}V_{nm}{}^2\rho \tag{15}$$

where w_{nm} is the radiationless-transition rate from $|2\rangle$ or $|1\rangle$ to equal energy levels, $\hbar = h/2\pi$ (h is Planck's constant), V_{nm} is a matrix element, and ρ is a density of vibrational states. The ratio of the VER rate from $|2\rangle$ to that from $|1\rangle$, w_2/w_1, was calculated by using experimental values. The total decay times from $|2\rangle$ and $|1\rangle$ are $w_2 = k_{21} + k_{20} = 1.90$ ps^{-1} and $w_1 = k_{10} = 0.54$ ps^{-1}, respectively. Therefore, we obtained $(w_2/w_1)_{exp} = 3.5$. On the other hand, w_2/w_1 becomes

$$\frac{w_2}{w_1} = \frac{\rho_2}{\rho_1} \tag{16}$$

when $V_{2m} = V_{1m}$ is assumed in eq 15. By direct counting combinations of vibrational modes in S_1 perylene, ρ_1 and ρ_2 can be estimated. The vibrational modes were computed with the CIS method included in WinMOPAC Version2.0 (Fujitsu). Because fwhm of the excitation pulse was 80 fs, the energy uncertainty width of the final-state manifold is 418 cm^{-1}. Therefore, ρ_1 is calculated as $\rho_1 = 858$/cm^{-1} at $\Delta\tilde{\nu} = 1465 \pm 209$ cm^{-1}, where $\Delta\tilde{\nu}$ is an excess vibrational energy, and $\rho_2 = 582721$/cm^{-1} at $\Delta\tilde{\nu} = 2897 \pm 209$ cm^{-1}. From eq 16 $(w_2/w_1)_{cal} = 679$ is calculated under the condition that $V_{2m} = V_{1m}$.

This large disagreement of w_2/w_1 between experimental and theoretical values may be attributed to the false of the assumption that the matrix elements of $|2\rangle$ and $|1\rangle$ are equal to each other, $V_{2m} = V_{1m}$. In fact, every matrix element has different

values depending on the combinations of initial and final states. However, each matrix element is unable to be obtained. Hence, we tried to estimate an average value of matrix elements $\langle V \rangle$ by using the Siebrand−Fourmann approximation,[24−26] in which the matrix elements vary not with combinations between the vibrational modes but with the overall difference between the vibrational quantum numbers, Δv_{total}, of interacting states. Fourmann et al. have used this approximation for isolated perylene under jet-cooled conditions where VER is clearly divided into the intra- and the intermolecular processes. Our experiments were, on the contrary, carried out in solution, in which the intramolecular process competes with the intermolecular process. Can we apply the Siebrand−Fourmann model to the system of perylene in solution? In this study, we have found that the VER time of PD is faster than that of perylene due to an increase in density of states by the carbonic-acid chain. Most of the observed VER in a few picoseconds region, therefore, would be considered as the intramolecular process. This reason leads us to try to use the Siebrand−Fourmann approximation for the system of perylene in solution.

Briefly, for every combination between initial and final states, all Δv_{total} were defined as

$$\Delta v_{\text{total}} = \sum_{k=1}^{90} [v_k^{\text{i}} + v_k^{\text{f}}] = 2, 3, 4, ... \qquad (17)$$

where v_k^{i} is the vibrational quantum number of kth vibrational mode in the initial state and v_k^{f} is that in the final state. For $\Delta v_{\text{total}} = l$ the mean value of matrix elements is given by

$$\langle V(l) \rangle = V_0 \alpha^{l-2} \qquad (3 \le l, 0 < \alpha < 1) \qquad (18)$$

where V_0 and α are the parameters to be determined by fitting the experimental data. The total change in vibrational quantum numbers should be larger than 2 because anharmonic coupling between two fundamentals ($l = 2$) may be neglected. As Δv_{total} increases, the matrix element becomes smaller in this expression. By substituting the matrix element of the Siebrand−Fourmann approximation (eq 18) into Fermi's golden rule, eq 15 may be written in the form

$$w = \frac{2\pi}{\hbar} \sum_l V_0^2 \alpha^{2(l-2)} \rho(l) \qquad (3 \le l) \qquad (19)$$

The densities of vibrational states relating to three transitions ($|2\rangle \rightarrow |1\rangle$, $|1\rangle \rightarrow |0\rangle$ and $|2\rangle \rightarrow |0\rangle$) were calculated, respectively. For $|2\rangle \rightarrow |1\rangle$ transition, final states are vibrational levels in which $|1\rangle$ is always excited (Figure 6a). For $|1\rangle \rightarrow |0\rangle$ and $|2\rangle \rightarrow |0\rangle$ transitions, final states are vibrational levels in which $|1\rangle$ is not excited (Figure 6b,c). The calculated densities of vibrational states are summarized in Table 2 and are plotted against Δv_{total} in Figure 7.

The density of vibrational states of the $|2\rangle \rightarrow |1\rangle$ transition is a little smaller than that of the $|1\rangle \rightarrow |0\rangle$ transition, which corresponds well with the experimental result that the VER rate of $|2\rangle \rightarrow |1\rangle$ is a little slower than that of $|1\rangle \rightarrow |0\rangle$. Though the density of vibrational states of $|2\rangle \rightarrow |0\rangle$ is much larger than the others, the VER rate of $|2\rangle \rightarrow |0\rangle$ is only 3−4 times faster than the others. These indicate that quantitative discussion of the VER rate is difficult only on the basis of the density of vibrational states estimated by the direct-counting method.

As mentioned earlier, in eq 19 V_0 and α are the variables that have to be determined from experiment. Equation 19 is

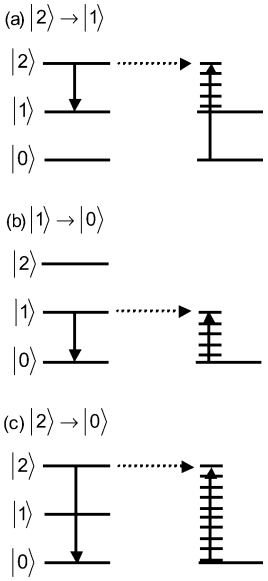

Figure 6. Schematic representation of radiationless transitions related to (a) $|2\rangle \rightarrow |1\rangle$, (b) $|1\rangle \rightarrow |0\rangle$, and (c) $|2\rangle \rightarrow |0\rangle$. (a) Final states are vibrational levels in which $|1\rangle$ is always excited; (b) and (c) final states are vibrational levels in which $|1\rangle$ is not excited.

TABLE 2: Density of Vibrational States (a) $|2\rangle \rightarrow |1\rangle$, (b) $|1\rangle \rightarrow |0\rangle$, and (c) $|2\rangle \rightarrow |0\rangle$

	ρ//cm^{-1}		
Δv_{total}	(a) $\|2\rangle \rightarrow \|1\rangle$	(b) $\|1\rangle \rightarrow \|0\rangle$	(c) $\|2\rangle \rightarrow \|0\rangle$
3	0.04	1.4	0.03
4	1.4	10	0.7
5	9.6	34	36
6	31	67	420
7	60	98	2242
8	85	114	7212
9	97	113	16239
10	96	102	28201
11	84	84	40385
12	70	66	50036
13	54	50	55543
14	41	37	56684
15	30	26	54225
16	21	18	49345
17	15	13	43194
18	10	8.5	36684
19	6.6	5.7	30418
20	4.4	3.7	24747
21	2.8	2.4	19822
22	1.8	1.5	15676
23	1.1	0.9	12262
24	0.7	0.5	9502
25	0.4	0.3	7301
total	721	858	582001

rewritten as

$$\frac{wh}{(2\pi V_0)^2} = \rho(3)\alpha^2 + \rho(4)\alpha^4 + \rho(5)\alpha^6 + \rho(6)\alpha^8 + ... \qquad (20)$$

To determine the V_0 and α values, eq 20 is divided into two as follows:

$$C = \frac{wh}{(2\pi V_0)^2} \qquad (21)$$

and

$$C = \rho(3)\alpha^2 + \rho(4)\alpha^4 + \rho(5)\alpha^6 + \rho(6)\alpha^8 + ... \qquad (22)$$

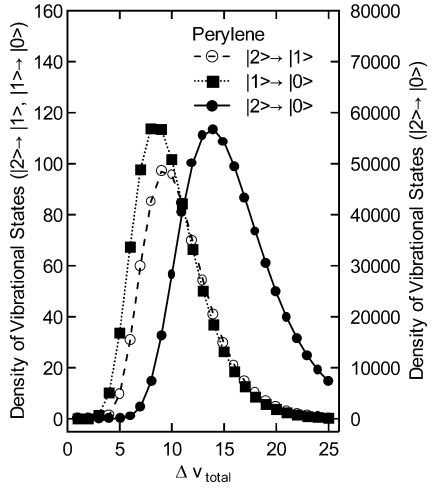

Figure 7. Calculated results of the densities of vibrational states with respect to three transitions for $|2\rangle \rightarrow |1\rangle$ (open circles), $|1\rangle \rightarrow |0\rangle$ (filled squares), and $|2\rangle \rightarrow |0\rangle$ (filled circles).

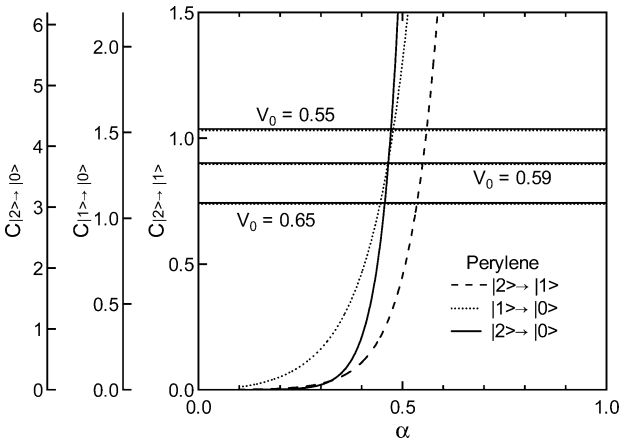

Figure 8. Dashed, dotted, and solid curves show eq 22 for the $|2\rangle \rightarrow |1\rangle$, $|1\rangle \rightarrow |0\rangle$, and $|2\rangle \rightarrow |0\rangle$ transitions, respectively. Dashed, dotted, and solid lines show eqs 23−25 with indicated V_0, respectively. α is determined from a cross point between the curve and line of the same forms.

Figure 8 depicts eq 22 for the $|2\rangle \rightarrow |1\rangle$, $|1\rangle \rightarrow |0\rangle$, and $|2\rangle \rightarrow |0\rangle$ transitions. According to eq 21, C is scaled as a function of V_0 by the following equations.

$$C_{|2\rangle\rightarrow|1\rangle} = \frac{0.37 \times 10^{12} \times 3.34 \times 10^{-11}}{(2\pi V_0)^2} \tag{23}$$

$$C_{|1\rangle\rightarrow|0\rangle} = \frac{0.54 \times 10^{12} \times 3.34 \times 10^{-11}}{(2\pi V_0)^2} \tag{24}$$

and

$$C_{|2\rangle\rightarrow|0\rangle} = \frac{1.53 \times 10^{12} \times 3.34 \times 10^{-11}}{(2\pi V_0)^2} \tag{25}$$

From Figure 8 we have found $V_0 = 0.59$ cm^{-1} and $046 < \alpha < 0.55$. Fourmann et al. estimated $V_0 = 0.65$ cm^{-1} and $\alpha = 0.3$ under the assumption that the VER rate was 2×10^{11} s^{-1} for 3000 cm^{-1} excess energy.[24] Considering the difference in experimental conditions such as gas phase and liquid phase, our V_0 and α are in reasonable agreement with the Fourmann's results.

TABLE 3: Transient Vibrational Temperatures

	perylene		PD	
time/ps	T_{10}/K	T_{20}/K	T_{10}/K	T_{20}/K
1.0	1190	2550	1020	1640
1.2	1140	1970	960	1390
1.4	1080	1670	890	1220
1.6	1030	1380	820	1090
1.8	980	1150	780	960
2.0	950	950	730	790
2.2	910	800	690	540
2.4	880	670	650	
2.6	850	550	630	
2.8	810		610	
3.0	790		590	
3.5	730		550	
4.0	680		520	
5.0	590		460	
6.0	540		390	
7.0	510		330	
8.0	490			

3.6. Transient Thermal Equilibrium Process. To discuss the energy flow in ν_7 mode, transient vibrational temperatures were calculated at each time by the following equation:

$$T_{mn} = \frac{\Delta E_{mn}}{k \ln(p_n/p_m)} \tag{26}$$

where T_{mn} is the vibrational temperature measured between $v' = m$ and n levels ($m > n$), ΔE_{mn} is a difference of vibrational energy between $v' = m$ and n, and p_m and p_n are the vibrational populations of $v' = m$ and n, respectively. The vibrational temperatures, T_{10} and T_{20}, at each delay time are summarized in Table 3. In the early time stages T_{20} is higher than T_{10}. T_{20} drops faster than T_{10}, and then T_{20} is equal to T_{10} at ∼2.0 ps both for perylene and for PD. Therefore, "intramode" thermal equilibrium appears to be achieved at ∼2.0 ps after photoexcitation. However, T_{20} continues to drop faster than T_{10} after that time, which would suggest that the "intramode" thermal equilibrium in the ν_7 mode is incomplete until the vibrational temperature is eventually equal to solvent temperature or room temperature. This experimental result can be explained by the rate equation of VER. From eqs 7 and 8,

$$\frac{N_1}{N_2} = \frac{k_{21}}{(k_{21} + k_{20}) - k_{10}}[1 - e^{\{(k_{21}+k_{20})-k_{10}\}t}] \tag{27}$$

When $k_{21} + k_{20} < k_{10}$, the ratio, N_1/N_2, approaches a constant value at a later time, which results in the "intramode" thermal equilibrium in the ν_7 mode. On the other hand, when $k_{21} + k_{20} > k_{10}$, the ratio continues to increase with time, and the "intramode" thermal equilibrium in the ν_7 mode is not achieved until the vibrational temperatures, T_{10} and T_{20}, return to room temperature. Our experimental result is the latter case.

From the viewpoint of the excitation-energy flow, it is still meaningful that the transient vibrational temperatures, T_{10} and T_{20}, are compared with the temperature at an "intermode" thermal equilibrium though the "intramode" thermal equilibrium in the ν_7 mode is not established while the vibrational temperature is higher than room temperature. The relation between excess vibrational energy ΔE and transient vibrational temperature T_t at the "intermode" thermal equilibrium calculated on

the assumption that ΔE is statistically distributed among all the vibrational modes is given by

$$\sum_{i=1}^{3N-6} \frac{h\nu_i \exp(-h\nu_i/kT_t)}{1-\exp(-h\nu_i/kT_t)} = \Delta E + \sum_{i=1}^{3N-6} \frac{h\nu_i \exp(-h\nu_i/kT_r)}{1-\exp(-h\nu_i/kT_r)} \quad (28)$$

where $h\nu_i$ is the vibrational energy of an *i*th vibrational mode and T_r is room temperature. The intramolecular vibrational temperatures at thermal equilibrium are calculated to be 428 K for perylene and 361 K for PD, by using the vibrational modes calculated by WinMOPAC Version 2.0 (Fujitsu) with the PM3 Hamiltonian, when the excess vibrational energy are equipartitioned over all the vibrational modes. These calculated statistical temperatures are very close to the experimentally obtained temperatures, 490 K at 8.0 ps for perylene and 390 K at 6.0 ps for PD (Table 3), indicating that the full intramolecular (both intra- and intervibrational modes) thermal equilibrium is almost completed at these delay times. However, the experimental values of 950 K at 2.0 ps for perylene and of 730 K at 2.0 ps for PD (Table 3) [at these times the apparent "intramode" thermal equilibrium is completed (this is not a "true equilibrium" as mentioned above)] are higher than the theoretical values obtained by assuming the equipartitioning of the excess vibrational energy over all the $3N - 6$ vibrational modes. This means that the "intermode" thermal equilibrium is not completed even after the "intramode" thermal equilibrium is done. In addition, the "intermode" equilibrium temperature was calculated on the assumption that IVR occurs initially only to, for example, FC-active symmetric a_g modes for perylene. In this case, the intramolecular vibrational temperature is calculated as $T_t = 900$ K, which is very close to the experimental value, $T_t = 950$ K at 2.0 ps. This result might indicate that the excess vibrational energy flows only to a_g modes during the initial IVR process, though further study is necessary. A similar calculation was not carried out on PD, because the classification of (pseudo)vibrational symmetry is very tedious in PD. Sension et al. have also reported such localization of an excess vibrational energy to FC active modes for S_0 *trans*-stilbene in hexane.[6]

4. Conclusion

We have investigated VER of S_1 perylene and S_1 PD in MTHF after photoexcitation with an excess vibrational energy of $\sim$2800 cm^{-1} ($v' = 2$ level of ring-breathing mode) by using the FC analysis of femtosecond time-resolved fluorescence spectra. From the results of the FC analysis we have shown that (1) the vibrational population at $v' = 2$ both for perylene and for PD survives even in a few picoseconds time scale following photoexcitation and (2) VER takes place via not only $|2\rangle \rightarrow |1\rangle$ followed by $|1\rangle \rightarrow |0\rangle$ successively but also $|2\rangle \rightarrow |0\rangle$ directly. An average-matrix-element treatment proposed by Fourmann et al.[24] was employed to account for these relaxation times in the Fermi's golden rule. Our results in solution were in reasonable agreement with the Fourmann's analysis for fluorescence spectra of perylene in supersonic jet. We have also concluded that (3) the "intramode" thermal equilibriums in the ν_7 mode both for perylene and for PD are not established while the vibrational temperature is higher than room temperature because the total relaxation rate from $|2\rangle$ is faster than that from $|1\rangle$. Further study is, however, required to conclude whether this result is extended to other vibrational modes in general.

In the present paper we limited ourselves to describe slower IVR in the picoseconds region. The FC analysis on fluorescence spectra of perylene and PD in femtoseconds region is underway and will be reported in the near future.

Acknowledgment. This work was supported in part by Grants-in-Aid for Scientific Research from the Ministry of Education, Science, Sports, and Culture, Japan, to S.A. (Grant No. 14750648), to S.S. (Grant No. 14540461), and to I.Y. (Grant on Priority Areas (B) No. 729).

References and Notes

(1) Akimoto, S.; Yamazaki, T.; Yamazaki, I.; Osuka, A. *Chem. Phys. Lett.* **1999**, *309*, 177.
(2) Baskin, J. S.; Yu, H.-Z.; Zewail, A. H. *J. Phys. Chem. A* **2002**, *106*, 9837.
(3) Sato, S.; Kitagawa, T. *Appl. Phys. B* **1994**, *59*, 415.
(4) Mizutani, Y.; Uesugi, Y.; Kitagawa, T. *J. Chem. Phys.* **1999**, *111*, 8950.
(5) Mizutani, Y.; Kitagawa, T. *Bull. Chem. Soc. Jpn.* **2002**, *75*, 623.
(6) Sension, R. J.; Szarka, A. Z.; Hochstrasser, R. M. *J. Chem. Phys.* **1992**, *97*, 5239.
(7) Schultz, S. L.; Qian, J.; Jean, J. M. *J. Phys. Chem. A* **1997**, *101*, 1000.
(8) Nakabayashi, T.; Okamoto, H.; Tasumi, M. *J. Phys. Chem. A* **1998**, *102*, 9686.
(9) Akimoto, S.; Yamazaki, I.; Sakawa, T.; Mimuro, M. *J. Phys. Chem. A* **2002**, *106*, 2237.
(10) Yamaguchi, S.; Hamaguchi, H. *Chem. Phys. Lett.* **1994**, *227*, 255.
(11) Sarkar, N.; Takeuchi, S.; Tahara, T. *J. Phys. Chem. A* **1999**, *103*, 4808.
(12) Ohta, K.; Kang, T. J.; Tominaga, K.; Yoshihara, K. *Chem. Phys.* **1999**, *242*, 103.
(13) Kasajima, T.; Akimoto, S.; Sato, S.; Yamazaki, I. *Chem. Phys. Lett.* **2003**, *375*, 227.
(14) Ohmine, I. *J. Chem. Phys.* **1986**, *85*, 3342.
(15) Nagaoka, M.; Okuno, Y.; Yamabe, T. *J. Phys. Chem.* **1994**, *98*, 12506.
(16) Meyer, Y. H.; Plaza, P. *Chem. Phys.* **1995**, *200*, 235.
(17) Jiang, Y.; Blanchard, G. J. *J. Phys. Chem.* **1994**, *98*, 9411.
(18) Jiang, Y.; Blanchard, G. J. *J. Phys. Chem.* **1995**, *99*, 7904.
(19) Goldie, S. N.; Blanchard, G. J. *J. Phys. Chem. A* **1999**, *103*, 999.
(20) Goldie, S. N.; Blanchard, G. J. *J. Phys. Chem. A* **2001**, *105*, 6785.
(21) Smalley, R. E. *J. Phys. Chem.* **1982**, *86*, 3504.
(22) Smith, W. L. *J. Phys. B* **1968**, *1*, 89.
(23) Yamasaki, K.; Taketani, F.; Tomita, S.; Sugiura, K.; Tokue, I. *J. Phys. Chem. A* **2003**, *107*, 2442.
(24) Fourmann, B.; Jouvet, C.; Tramer, A.; Le Bars, J. M.; Millie, Ph. *Chem. Phys.* **1985**, *92*, 25.
(25) Siebrand, W. *J. Chem. Phys.* **1967**, *46*, 440.
(26) Siebrand, W. *J. Chem. Phys.* **1967**, *47*, 2411.